Solid State Ionics 263 (2014) 57–61

Contents lists available at ScienceDirect

Solid State Ionics

journal homepage: www.elsevier.com/locate/ssi

Conductivity of $70Li_2S\cdot30P_2S_5$ glasses and glass–ceramics added with lithium halides

Satoshi Ujiie [a,b], Toru Inagaki [b], Akitoshi Hayashi [a], Masahiro Tatsumisago [a,*]

[a] *Department of Applied Chemistry, Graduate School of Engineering, Osaka Prefecture University, 1-1 Gakuencho, Naka-ku, Sakai, Osaka 599-8531, Japan*
[b] *Energy Use R&D Center, The Kansai Electric Power Co., Inc., 11-20-3 Nakoji, Amagasaki, Hyogo 661-0974, Japan*

ARTICLE INFO

Article history:
Received 2 December 2013
Received in revised form 11 May 2014
Accepted 12 May 2014
Available online 5 June 2014

Keywords:
Solid electrolyte
Glass
Glass–ceramic
Lithium ion conductivity
Lithium halide

ABSTRACT

Glasses and glass–ceramics of $(100 - y)(0.7Li_2S\cdot0.3P_2S_5)\cdot yLiX$ (mol%) ($0 \le y \le 20$, X = F, Cl, Br, and I) were synthesized using mechanical milling and subsequent heat treatment. The conductivities of glasses added with LiBr and LiI improved with increasing lithium halide contents. Larger halide ions produced higher conductivity. All glass–ceramic samples contained $Li_7P_3S_{11}$ crystals. The $Li_7P_3S_{11}$ crystal crystallinity was degraded with increasing lithium halide content. The composition dependence of conductivities differed depending on the added lithium halides. Incorporation of LiBr was most effective for increasing the $70Li_2S\cdot30P_2S_5$ glass–ceramic conductivity.

1. Introduction

Lithium ion batteries with high energy density are important components of portable electronic equipment such as mobile phones and laptop computers. Large capacity cells are also put into practical use and are adopted as power supplies for electric vehicles. Large cells are anticipated for use in electric power grids with the aim of power storage and load-frequency control. The high energy density of lithium ion batteries is attributable to the high voltage of the cells. Liquid electrolytes containing organic solvents are used in lithium ion batteries because they are stable under the high voltage of the cells. However, organic electrolytes pose a risk of combustion because of their flammability. All-solid-state lithium batteries using solid electrolytes are anticipated to resolve persistent safety problems.

Non-flammable inorganic electrolytes, especially oxide and sulfide glasses and glass–ceramics, are attractive as electrolytes of all-solid-state lithium batteries because they show high lithium ion conductivity [1–14]. Oxide glasses in the binary Li_2O–B_2O_3 system synthesized by melt quenching have poor conductivity of 10^{-7} S cm^{-1} at room temperature [1]. However, the addition of lithium halides to the glasses increases their conductivity. Ternary glass of $23Li_2O\cdot42B_2O_3\cdot35LiCl$ (mol%) shows conductivity of 10^{-6} S cm^{-1} at room temperature [2]. The conductivity increases concomitantly with increasing lithium halide content. Given equal lithium halide contents, the larger the halide ion is, the higher the conductivity is. Sulfide glasses in the binary Li_2S–B_2S_2 system synthesized by melt quenching have high conductivity of 10^{-4} S cm^{-1} at room temperature [3,4]. Incorporation of LiI into the Li_2S–B_2S_3 glasses enhances conductivity up to 1.7×10^{-3} S cm^{-1} at the composition of $30Li_2S\cdot26B_2S_3\cdot44LiI$ [3]. Glasses in the Li_2S–SiS_2 system also have conductivity of 10^{-4} S cm^{-1} at room temperature [5–7]. The conductivity of Li_2S–SiS_2 glasses is increased by the addition of lithium halides. The conductivity of the glasses added with LiI is higher than that of glasses added with LiBr of the same concentration [5]. In fact, $42Li_2S\cdot28SiS_2\cdot30LiI$ glass has conductivity of 1.8×10^{-3} S cm^{-1} [6]. Glasses in the Li_2S–P_2S_5 system prepared by melt quenching have conductivity of 10^{-4} S cm^{-1} at room temperature [4,8,9]. The addition of LiI to Li_2S–P_2S_5 glasses enhances conductivity just as it does with the other glasses. $37Li_2S\cdot18P_2S_5\cdot45LiI$ glass shows conductivity of 1×10^{-3} S cm^{-1} [8,9]. The Li_2S–P_2S_5 glasses are synthesized by mechanical milling [10]. The Li_2S–P_2S_5 glasses obtained by mechanical milling show roughly equal conductivities of melt-quenched glasses. In addition, the glass-forming range achieved by mechanical milling is extended to higher Li_2S contents than that by melt quenching. Sulfide glass–ceramics in the Li_2S–P_2S_5 system were prepared by crystallization of the milled glasses [11–13]. Crystal phases precipitated from the Li_2S–P_2S_5 glasses differ depending on the composition. The $80Li_2S\cdot20P_2S_5$ glass–ceramic, which has a thio-LISICON II analog phase as a primary crystal, shows conductivity of 1.3×10^{-3} S cm^{-1} at 25 °C [12,13]. The $75Li_2S\cdot25P_2S_5$ glass–ceramic has a thio-LISICON III analog phase and conductivity of 3.2×10^{-4} S cm^{-1} [12,13]. The $70Li_2S\cdot30P_2S_5$ glass–ceramic containing $Li_7P_3S_{11}$ crystal has high conductivity of 5.2×10^{-3} S cm^{-1} [14,15]. As sulfide crystals containing halide, lithium

---

* Corresponding author.
E-mail address: tatsu@chem.osakafu-u.ac.jp (M. Tatsumisago).

http://dx.doi.org/10.1016/j.ssi.2014.05.002
0167-2738/

argyrodites of Li_6PS_5I, Li_6PS_5Br, and Li_6PS_5Cl were synthesized [16,17]. Li_6PS_5Cl showed high conductivity of 1.3×10^{-3} S cm^{-1}.

As described above, incorporation of lithium halides into binary glasses is effective for enhancing the lithium ion conductivity. Conductivities depending on added lithium halides were investigated for Li_2O–B_2O_3 and Li_2S–SiS_2 glasses. The influence of added LiI on the conductivity was studied for Li_2S–P_2S_5 glass. However, the influence of other lithium halides has not been clarified for Li_2S–P_2S_5 glass. Moreover, the conductivities and structures of Li_2S–P_2S_5 glass–ceramics added with lithium halides have not been investigated. Therefore we undertook research into Li_2S–P_2S_5 glasses and glass–ceramics added with lithium halides. The properties of Li_2S–P_2S_5–LiI and Li_2S–P_2S_5–LiBr glasses and glass–ceramics had already been reported [18–20].

In this study, conductivities and structures depending on added lithium halides were discussed for ternary glasses and glass–ceramics of $70Li_2S \cdot 30P_2S_5$ added with LiF, LiCl, LiBr, and LiI. The composition of $70Li_2S \cdot 30P_2S_5$ was selected because the glass–ceramic of $70Li_2S \cdot 30P_2S_5$ has the highest conductivity in the binary Li_2S–P_2S_5 system. The ternary glasses and glass–ceramics were prepared. Their conductivities and crystalline phases were examined. The differences of the properties were studied from the perspective of added halides.

2. Experimental

$(100 - y)(0.7Li_2S \cdot 0.3P_2S_5) \cdot yLiX$ (mol%) ($0 \le y \le 20$, X = F, Cl, Br, and I) glasses were obtained by mechanical milling. Reagent-grade Li_2S (99.9%; Nippon Chemical Industrial Co.), P_2S_5 (99%; Aldrich), LiF (99.99%; Aldrich), LiCl (99.998%; Aldrich), LiBr (99.999%; Aldrich), and LiI (99.99%; Aldrich) were used as starting materials. They were mixed in an agate mortar for 10 min and put into a 45 ml ZrO_2 pot with 500 4-mm-diameter ZrO_2 balls. The pot was set in a planetary ball mill apparatus (Pulverisette 7; Fritsch GmbH). Then mechanical milling was performed at 500 rpm for 10 h. All processes were conducted in a dry Ar atmosphere. Glass–ceramic samples were prepared by heating the glass samples.

Differential thermal analyses (DTA) were performed using a thermal analyzer (Thermo-plus 8120; Rigaku Corp.) to observe crystallization temperatures. The glass samples, which were sealed in Al pans in an Ar-filled glove box, were heated at 10 °C min^{-1} under N_2 gas flow up to 400 °C. X-ray diffraction (XRD) measurements (CuKα) were conducted using a diffractometer (SmartLab; Rigaku Corp.) to identify crystal phases of the glass samples and the glass–ceramic samples. Ionic conductivities were measured for the pelletized samples pressed under 360 MPa. The pellet diameter and thickness were, respectively, 10 mm and about 1.5 mm. Carbon paste was painted as electrodes on both faces of the pellets. Then stainless steel disks were attached to the pellets as current collectors. The prepared cell was sealed in a silica glass tube. Then AC impedance measurements were conducted under dry Ar gas flow using an impedance analyzer (1260; Solartron). The frequency range and the applied voltage were, respectively, 10 Hz to 8 MHz and 50 mV. The AC impedance measurements were conducted at 25 °C for the glass samples. Then the pellets were heated to above the crystallization temperatures to obtain glass–ceramics. The impedances of glass–ceramic samples were measured after cooling the pellets to 25 °C.

3. Results and discussion

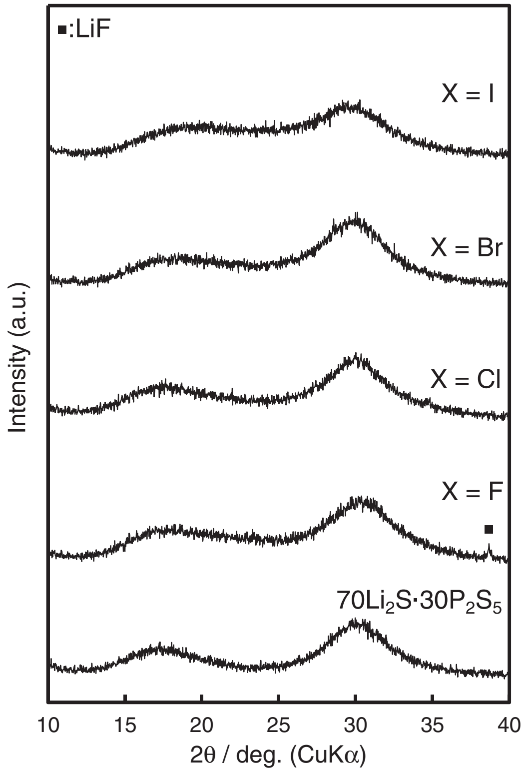

Fig. 1. XRD patterns of the $90(0.7Li_2S \cdot 0.3P_2S_5) \cdot 10LiX$ samples prepared using mechanical milling, and of the $70Li_2S \cdot 0.3P_2S_5$ glass.

Figs. 1 and 2 respectively portray XRD patterns of the $90(0.7Li_2S \cdot 0.3P_2S_5) \cdot 10LiX$ and $80(0.7Li_2S \cdot 0.3P_2S_5) \cdot 20LiX$ samples (X = F, Cl, Br, and I) prepared using mechanical milling. The XRD pattern of $70Li_2S \cdot 30P_2S_5$ is also depicted in the figures. Halo patterns were observed for all samples. A weak diffraction peak attributable to LiF crystals remained in the XRD patterns of the $90(0.7Li_2S \cdot 0.3P_2S_5) \cdot 10LiF$ and $80(0.7Li_2S \cdot 0.3P_2S_5) \cdot 20LiF$ samples. Weak diffraction peaks attributable to LiCl crystals were observed in the XRD patterns of the $80(0.7Li_2S \cdot 0.3P_2S_5) \cdot 20LiCl$ sample. No crystal peak remained in the

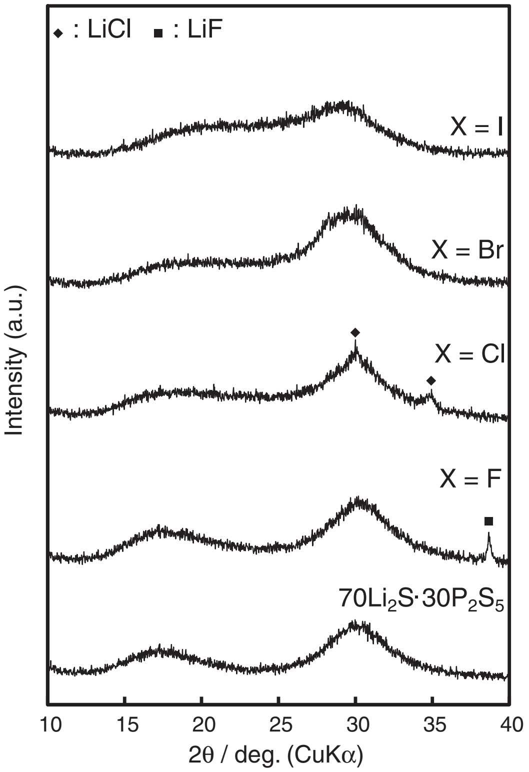

Fig. 2. XRD patterns of the $80(0.7Li_2S \cdot 0.3P_2S_5) \cdot 20LiX$ samples prepared using mechanical milling, and of the $70Li_2S \cdot 0.3P_2S_5$ glass.